3D MODELING OF DAMAGE GROWTH AND DUCTILE CRACK PROPAGATION USING ADAPTIVE FEM TECHNIQUE

HAMID MOSLEMI* AND AMIR R. KHOEI†

* Department of Civil Engineering, Engineering Faculty
Shahed University
P.O. Box .18155/159, Tehran, Iran
e-mail: h.moslemi@shahed.ac.ir

† Center of Excellence in Structures and Earthquake Engineering
Department of Civil Engineering, Sharif University of Technology,
P.O. Box. 11365-9313, Tehran, Iran
e-mail: arkhoei@sharif.edu

Key words: Damage Mechanics, Crack Initiation, Crack Closure, Adaptive Mesh Refinement, Weighted SPR Technique.

Abstract. In this paper, the continuum damage mechanics model originally proposed by Lemaitre [1] is presented through an adaptive finite element method for three-dimensional ductile materials. The macro-crack initiation–propagation criterion is used based on the distribution of damage variable in the continuum damage model. The micro-crack closure effect is incorporated to simulate the damage evolution more realistic. The Zienkiewicz-Zhu posteriori error estimator is employed in conjunction with a weighted superconvergence patch recovery (SPR) technique at each patch to improve the accuracy of error estimation and data transfer process. Finally, the robustness and accuracy of proposed computational algorithm is demonstrated by a 3D numerical example.

1 INTRODUCTION

The fracture of ductile materials is the consequence of a progressive damaging process and considerable plastic deformation usually precedes the ultimate failure. The numerical prediction of damage evolution and crack initiation–propagation can be described by the means of continuum damage approach. The continuum damage mechanics was originally developed to describe the creep rupture. It was first introduced by Kachanov [2] to describe the effects of an isotropic distribution of spherical voids on plastic flow. Gurson [3] proposed a model based on the theory of elasto-plasticity for ductile damage where the (scalar) damage variable was obtained from the consideration of microscopic spherical voids embedded in an elasto-plastic matrix. It was shown that the theory is particularly suitable for representation of the behavior of porous metals. Lemaitre [1] proposed a micro-mechanical damage model to simulate the physical process of void nucleation, growth and coalescence using continuum mechanics. Lemaitre and Chaboche [4] pointed out the fracture as the ultimate consequence of material degradation process. The superconvergent patch recovery (SPR) method was first introduced by Zienkiewicz and Zhu [5] in linear elastic problems. The technique was applied in nonlinear analysis by Boroomand and Zienkiewicz [6], in which the strain was recovered by SPR in elasto-plasticity problems. An extension of SPR technique to 3D plasticity problems was presented by Khoei and Gharehbaghi [7]. A modified–SPR technique was applied by Khoei et al. [8] for simulation of crack propagation, in which the polynomial function was replaced by singular terms of analytical solution of crack problems in the process of recovery solution. The technique was improved by Moslemi and Khoei [9] and Khoei et al. [10] to estimate a more realistic error in LEFM problems and cohesive zone models by applying the weighting function for various sampling points. In the present paper, an adaptive finite element method is presented based on the weighted–SPR technique to model the damage of ductile material in 3D problems.

2 NONLINEAR DAMAGE MODEL

Damage in materials is mainly the process of initiation and growth of micro-cracks and cavities. Continuum damage mechanics discusses systematically the effects of damage on the mechanical properties of materials and structures as well as the influence of external conditions and damage itself on the subsequent development of damage. In this study, this nonlinear interaction is investigated via the Lemaitre damage constitutive model. In order to describe the internal degradation of solids within the framework of the continuum mechanics theory, new variables intrinsically connected with the internal damage process need to be introduced in addition to the standard variables. Variables of different mathematical nature possessing different physical meaning have been employed in the description of damage under various circumstances. The damage variable used here is the relative area of micro-cracks and intersections of cavities in any plane oriented by its normal n as

$$D_{(\mathrm{n})} = \frac{S_{\Phi}}{S} \tag{1}$$

where S_{Φ} is the area of micro-cracks and intersections and S is the total area of the cross section. It is assumed that micro-cracks and cavities are distributed uniformly in all directions. In the isotropic case, the damage variable is adopted as a scalar. The behavior of damaged material is governed by the principle of strain equivalence which states that the strain behavior of a damaged material is represented by constitutive equations of the virgin material (without damage) in the potential of which the stress is simply replaced by the effective stress. By this assumption the effective stress tensor is related to the true stress tensor by

$$\boldsymbol{\sigma}_{eff} = \frac{1}{1-D}\boldsymbol{\sigma} \tag{2}$$

In Lemaitre damage model the evolution of damage variable is assumed to be given by

$$\dot{D} = \begin{cases} 0 & \varepsilon_{eq}^{p} \le \varepsilon_{D}^{p} \\ \dot{\gamma}\dfrac{1}{1-D}\left(\dfrac{-Y}{r}\right)^{s} & \varepsilon_{eq}^{p} > \varepsilon_{D}^{p} \end{cases} \tag{3}$$

where *r* and *s* are material and temperature-dependant properties, $\varepsilon_{eq}^{p}=\sqrt{2/3\|\boldsymbol{\varepsilon}^{p}\|}$ is equivalent plastic strain, $\dot{\gamma}$ is the plastic multiplier and is equal to the rate of equivalent plastic strain and ε_{D}^{p} is threshold damage where damage growth starts only at this critical value. *Y* is called damage energy release rate and is expanded by using the inverse of the elastic stress-strain law as

$$\begin{aligned} Y &= -\frac{1}{2(1-D)^2}\boldsymbol{\sigma}:[\mathbf{D}^e]^{-1}:\boldsymbol{\sigma} = -\frac{1}{2E(1-D)^2}[(1+\nu)\boldsymbol{\sigma}:\boldsymbol{\sigma}-\nu(tr\,\boldsymbol{\sigma})^2] \\ &= -\frac{q^2}{2E(1-D)^2}\left[\frac{2}{3}(1+\nu)+3(1-2\nu)\left(\frac{p}{q}\right)^2\right] \end{aligned} \tag{4}$$

where p is the hydrostatic stress and q is the equivalent von–Mises stress.As can be seen in above equation the damage rate depends on the stress state, plastic strain growth and instantaneous damage variable. The effect of damage variable on mechanical behavior of material is accounted in degradation of elastic modulus of material and its yield surface. Based on the equivalent strain principle this modification can be expressed as

$$\mathbf{D}_{eff}=(1-D)\mathbf{D}^e \tag{5}$$

$$\Phi=\sqrt{\frac{3}{2}}\frac{\|\mathbf{s}\|}{(1-D)}-[\sigma_Y^0+R(\varepsilon_{eq}^p)] \tag{6}$$

where $\mathbf{D}^e$ and $\mathbf{D}_{eff}$ are the elastic modulus of material before damage and after damage, respectively, $\boldsymbol{\Phi}$ is the modified yield surface, $\mathbf{s}$ is the deviatoric stress tensor and *R* is the isotropic plastic growth function.

2.1 Finite element implementation

The accuracy of the overall finite element scheme depends crucially on the accuracy of particular numerical algorithm adopted. This section describes a numerical procedure for integration of the Lemaitre damage elasto-plastic model presented in preceding section, based on the well-known two-step elastic predictor–plastic corrector method. At each Gauss point, the values of state variables including the stress tensor $\boldsymbol{\sigma}_n$, plastic strain tensor $\boldsymbol{\varepsilon}_n^p$, equivalent plastic strain $(\varepsilon_{eq}^p)_n$ and damage variable D_n are known at the start of interval, and for a given strain increment $\Delta\boldsymbol{\varepsilon}$, the value of variables are desired at the end of interval. At the first stage of computational algorithm the material behavior is assumed to be elastic, the yield surface at the end of interval can be then evaluated as

$$\Phi=\sqrt{\frac{3}{2}}\frac{\|\mathrm{s}_{n+1}\|}{(1-D_n)}-[\sigma_Y^0+R(\varepsilon_{eq}^p)_n] \tag{7}$$

If $\boldsymbol{\Phi}\le 0$, the assumed elastic behavior is correct and the damage variable and plastic strain remain unchanged. If $\boldsymbol{\Phi}>0$, the plastic corrector step must be applied to obtain the updated state variables by simultaneously establishing four equations consisting of the plastic flow equation, equivalent plastic strain growth equation, damage growth equation, and the yield surface equation as

$$\varepsilon_{n+1}^{p} = \varepsilon_{n}^{p} + \frac{\Delta\gamma}{1-D_{n+1}}\sqrt{\frac{3}{2}}\frac{\mathrm{s}_{n+1}}{\|\mathrm{s}_{n+1}\|} \tag{8}$$

$$(\varepsilon_{eq}^{p})_{n+1} = (\varepsilon_{eq}^{p})_{n} + \Delta\gamma \tag{9}$$

$$D_{n+1} = D_n + \Delta\gamma\frac{1}{1-D_{n+1}}\left(\frac{-Y_{n+1}}{r}\right)^{s} \tag{10}$$

$$\Phi = \sqrt{\frac{3}{2}}\frac{\|\mathrm{s}_{n+1}\|}{(1-D_{n+1})} - \left[\sigma_Y^0 + R\,(\varepsilon_{eq}^{p})_{n+1}\right] = 0 \tag{11}$$

The solution of these four nonlinear coupled equations simultaneously is a costly computational task. By performing relatively straightforward algebraic manipulations, the above system can be reduced to a single nonlinear algebraic equation for the plastic multiplier $\Delta\gamma$ expressed as

$$\omega(\Delta\gamma) - \omega_n + \frac{\Delta\gamma}{\omega(\Delta\gamma)}\left(\frac{-Y(\Delta\gamma)}{r}\right)^{s} = 0 \tag{12}$$

where ω is the integrity variable in contrast to damage variable and is evaluated by

$$\omega_{n+1} = 1 - D_{n+1} = \omega(\Delta\gamma) = \frac{3G\Delta\gamma}{\bar{q}_{n+1}^{trial} - \sigma_Y(R_n + \Delta\gamma)} \tag{13}$$

where $\bar{q}_{n+1}^{trial}$ is the von–Mises equivalent stress obtained in the elastic predictor step. The damage energy release rate is a function of $\Delta\gamma$ calculated by

$$Y(\Delta\gamma) = \frac{\left[\sigma_Y(R_n + \Delta\gamma)\right]^2}{6G} + \frac{\bar{p}_{n+1}^2}{2K} \tag{14}$$

where $\bar{p}_{n+1}$ is the elastic predicted hydrostatic pressure without damage effect. Equation (12) can be solved by an iterative method such as Newton-Raphson method. By computing the plastic multiplier, the updated state variables can be obtained using four basic equations.

2.2 Micro-crack closure effect

From the micromechanical view, the damage can be considered as the degradation of material properties due to the evolution of voids and micro-cracks. The Lemaitre damage model discussed in previous section, suffers from an important drawback, since the effect of hydrostatic stress is captured by the damage energy release rate Y with equal response in tension and compression. On the other hand, the micro-cracks which open in tensile stresses may partially close at a compression stress state. Hence, after having been damaged in tension, the material recovers its stiffness partially under compression. In this study, the stress tensor is decomposed into the positive and negative parts and the effect of compressive stress tensor is considered as a fraction of the effect of tensile stress tensor. In the process of decomposition, the stress tensor is first mapped to the principle directions to form a diagonal matrix with the principle stresses. This matrix is then decomposed to tensile and compressive stress tensors as

$$\boldsymbol{\sigma} = \boldsymbol{\sigma}^{+} + \boldsymbol{\sigma}^{-} \tag{15}$$

This decomposition is defined mathematically using the Macaulay bracket $\langle \ \rangle$ as

$$\boldsymbol{\sigma}^{+} = \begin{bmatrix} \langle \sigma_1 \rangle & 0 & 0 \\ 0 & \langle \sigma_2 \rangle & 0 \\ 0 & 0 & \langle \sigma_3 \rangle \end{bmatrix} \qquad \boldsymbol{\sigma}^{-} = -\begin{bmatrix} \langle -\sigma_1 \rangle & 0 & 0 \\ 0 & \langle -\sigma_2 \rangle & 0 \\ 0 & 0 & \langle -\sigma_3 \rangle \end{bmatrix} \tag{16}$$

The Macaulay bracket is a scalar function defined as

$$\langle a \rangle = \begin{cases} a & \text{if } a \geq 0 \\ 0 & \text{if } a < 0 \end{cases} \tag{17}$$

By decomposition of stress tensor, each component affects the damage energy release rate separately. The effect of tensile component given in Section 2 remains valid, but the compression component has a more moderate effect with an experimental reduction factor of h . This value is called as the crack closure effect constant and has the value in the range of $[0-1]$. Thus, the effect of compressive component of stress tensor can be superposed with the effect of tensile component of stress tensor by modifying equation (4) as

$$Y = -\frac{1}{2E(1-D)^2}\left[(1+\nu)\boldsymbol{\sigma}^{+} : \boldsymbol{\sigma}^{+} - \nu \langle tr\,\boldsymbol{\sigma} \rangle^2 \right] - \frac{h}{2E(1-hD)^2}\left[(1+\nu)\boldsymbol{\sigma}^{-} : \boldsymbol{\sigma}^{-} - \nu \langle -tr\,\boldsymbol{\sigma} \rangle^2 \right] \tag{18}$$

By modifying the value of damage energy release rate, the remaining parts of the procedure of original Lemaitre model will not be changed.

3 ADAPTIVE FINITE ELEMENT STRATEGY

In numerical analysis of FE solution, it is essential to introduce some measures of error and use adaptive mesh refinement to keep this error within prescribed bounds to ensure that the finite element method is effectively used for practical analysis. To automate this process, several adaptive finite elements have been implemented to obtain an optimal mesh. Due to the localized material deterioration in the damaged body problems, many elements will be severely distorted producing unacceptably inaccurate solutions and this optimization takes a more important and necessary role. In order to obtain an optimal mesh, in the sense of an equal solution quality, it is desirable to design the mesh such that the error contributions of the elements are equally distributed over the mesh. This criterion illustrates what parts of the discretized domain have to be refined/de-refined and what degree of mesh fineness is needed to maintain the solution error within the prescribed bounds. The plastic deformation of problem necessitates transferring all relevant variables from the old mesh to new one. In general, the procedure described above can be executed in four parts; an error estimation, an adaptive mesh refinement, an adaptive mesh generator, and the mapping of variables.

3.1 Error estimation using weighted SPR technique

In the error estimation process two main aims are followed: firstly, to determine the error for the chosen mesh and secondly, to reduce this error to a permissible value by an automatic adaptive remeshing. The discretization error for a state variable represents the difference between its exact and the finite element solutions. Thus, the error of typical state variable α can be defined by $e_\alpha = \alpha - \hat{\alpha}$, with α denoting the exact value of state variable and $\hat{\alpha}$ the value of state variable derived by a finite element solution. Since the exact value of state variables for nonlinear problems is not available, we use a recovered solution instead of exact ones and then approximate the error as the difference between the recovered values and those given directly by the finite element solution, i.e. $e_\alpha \approx \alpha^* - \hat{\alpha}$, where α^* denotes the recovered value of state variable α.

Since the damage variable plays an important role in predicting the crack initiation and crack growth, its accuracy is very crucial in this process. Thus, the error is estimated based on the damage variable D. In order to obtain an improved solution, the nodal smoothing procedure is performed using the weighted superconvergent patch recovery (WSPR) technique, which was originally proposed by Moslemi and Khoei [9] to simulate the crack growth in linear fracture mechanics. The objective of recovery of the finite element solution is to obtain the nodal values of damage variable D such that the smoothed continues field defined by the shape functions and nodal values is more accurate than that of the finite element solution. A procedure for utilizing the Gauss quadrature values is based on the smoothing of such values by a polynomial of order p in which the number of sample points can be taken as greater than the number of parameters in the polynomial. In this case, if we accept the superconvergence at certain points of each element, the computed values of damage variable have the superconvergent accuracy at all points within the element. Thus, the recovered solution of damage variable D^* can be obtained as

$$D^* = \mathbf{P}\mathbf{a} \tag{19}$$

where $\mathbf{a}$ is a vector of unknown parameters and $\mathbf{P}$ the polynomial base functions. Depending on the order of polynomial the technique is called as C0-SPR, C1-SPR, etc. It was shown by Khoei et al. [8] in crack growth problems that if the singular elements are used near the crack tip the modified–SPR technique, in which the polynomial function is replaced by the singular terms of analytical solution of crack problems leads to better results in the process of recovery solution. Since the isoparametric elements are employed here over the domain, the linear base functions are used for the recovery process. Hence, the vectors $\mathbf{P}$ and $\mathbf{a}$ are represented in their simplest form as

$$\mathbf{P} = \langle 1 , x , y , z \rangle \qquad \mathbf{a} = \langle a_1 , a_2 , a_3 , a_4 \rangle^T \tag{20}$$

The determination of the unknown parameters $\mathbf{a}$ can be made by performing a least square fit to the values of superconvergent, or sampling points. After finite element analysis, a patch is defined for each vertex node inside the domain by the union of elements sharing the node. At each node of interior patch center, the connected tetrahedral elements along with their nodes and Gauss points are obtained. The number of sampling points must be at least equal to number of parameters in the polynomial. In the standard SPR technique, all sampling points have similar properties in the patch, which may produce significant errors in the boundaries, particularly the edges of crack. In fact, for elements located on the boundaries, constraints and crack edges, which do not have enough sampling points, we need to use the sampling points of nearest patch. These new sampling points induce unreal value of damage variables in the patch and overestimate the value of error, which results in unreasonable mesh refinement in the boundaries of domain. Moslemi and Khoei [9] proposed the weighted–SPR technique by using different weighting parameters for sampling points of the patch. It results in more realistic recovered values at the nodal points, particularly near the crack tip and boundaries. Hence, if we have n sampling points in the patch with the coordinates (x_k, y_k, z_k), the function F needs to be minimized in this patch as

$$\begin{aligned} F(\mathbf{a}) &= \sum_{k=1}^{n} w_k \left[D_i^*(x_k, y_k, z_k) - \widehat{D}_i(x_k, y_k, z_k) \right]^2 \\ &= \sum_{k=1}^{n} w_k \left[\mathbf{P}(x_k, y_k, z_k)\mathbf{a} - \widehat{D}_i(x_k, y_k, z_k) \right]^2 \end{aligned} \tag{21}$$

In order to incorporate the effects of nearest sampling points in the recovery process, the weighting parameter is defined as $w_k = 1/r_k$, with r_k denoting the distance of sampling point from the vertex node which is under recovery. The minimization of function F with respect to $\mathbf{a}$ results in the unknown parameters $\mathbf{a}$ as

$$\mathbf{a} = \left(\sum_{k=1}^{n} w_k^2\, \mathbf{P}_k^T\, \mathbf{P}_k \right)^{-1} \sum_{k=1}^{n} \left[w_k^2\, \mathbf{P}_k^T\, \widehat{D}_i(x_k, y_k) \right] \tag{22}$$

It must be noted that the implementation of global coordinates may result in ill-conditioned coefficient matrix, hence it is preferred to use a local coordinate system in the patch. Once the components of the vector of unknown parameters $\mathbf{a}$ are determined, the damage variables at nodal points inside the patch are computed by substituting their coordinates in equation (19). These nodal values $\bar{\boldsymbol{D}}^*$ can be used to construct a continuous damage field over the entire domain at the next step, that is, for each element, the recovered damage variable is represented as an interpolation of nodal values using the standard shape functions $\mathbf{N}$ in finite element analysis as

$$D^* = \mathbf{N}\,\bar{\boldsymbol{D}}^* \tag{23}$$

The recovered damage variable obtained by above equation can be used to obtain a pointwise error in the domain. Since the pointwise error becomes locally infinite in critical points, such as crack tip, point constraint and point loads, the error estimator can be replaced by a global parameter using the norm of error defined as

$$\|e_D\| = \|D^* - \hat{D}\| = \left(\int_\Omega (D^* - \hat{D})^T (D^* - \hat{D}) \, d\Omega \right)^{\frac{1}{2}} \tag{24}$$

The above *L2* norm is defined over the whole domain Ω. The overall error can be related to each element error by

$$\|e_D\|^2 = \sum_{i=1}^{m} \|e_D\|_i^2 \tag{25}$$

with *i* denoting an element contribution and m the total number of elements. The distribution of error norm across the domain indicates which portions need refinement and which other parts need de-refinement, or coarsening elements.

3.2 Adaptive mesh refinement

Once the error estimator process has been achieved it needs to implement a technique by which the solution can be improved. Since the total error permissible must be less than a certain value, it is a simple matter to search the design field for a new solution in which the total error satisfies this requirement. The simplest process is based on an equal error distribution among all elements as with such equal error distribution the results are most economical. In fact, after remeshing each element must obtain the same error and the overall percentage error must be less than the target percentage error, i.e.

$$\theta = \frac{\|e_D\|}{\|\hat{D}\|} \le \theta_{\text{aim}} = \frac{\|e_D\|_{\text{aim}}}{\|\hat{D}\|} \tag{26}$$

where θ_{aim} is the prescribed target percentage error. Hence, the aim error at each element can be obtained as

$$\left(\|e_D\|_i \right)_{\text{aim}} = \frac{1}{\sqrt{m}} \|\hat{D}\| \; \theta_{\text{aim}} \tag{27}$$

The rate of convergence of local error depends on the order of elements. The higher-order elements show faster convergence to the aim error. Thus, such elements need less refinement and new element size depend on its error norm and its order. Thus, the new element size can be evaluated as

$$(h_i)_{\text{new}} = \left[\frac{\left(\|e_D\|_i \right)_{\text{aim}}}{\left(\|e_D\|_i \right)_{\text{old}}} \right]^{1/p} (h_i)_{\text{old}} \tag{28}$$

where *h* is the average element size and p is the order of element. To obtain the nodal element size, a simple averaging between elements joining a node is used. As the mesh tends progressively to be optimal with the error uniformly distributed between elements this theoretical rate of convergence appears very effective. The above technique can be coupled with an efficient mesh generator which allows the new mesh to be constructed according to a predetermined size distribution.

3.3 Data transfer operator

In the nonlinear FE analysis, the new mesh must be used starting from the end of previous load step since the solution is history-dependent in nonlinear problems. Thus, the state and internal variables need to be mapped from the old finite element mesh to the new one. The state variables consist of the nodal displacements and the internal variables, including the Cauchy stress tensor, the strain tensor, the plastic strain tensor and damage variable. Since these variables are transferred separately, it is important that the transfer of information from the old to new meshes is achieved with minimum discrepancy in equilibrium and constitutive relations. Hence, a minimum number of internal variables must be transferred and remaining variables are calculated by equilibrium and constitutive equations. In the case of internal variables which their values evaluated at the Gauss points of the old mesh, corresponding values at the Gauss points of the new mesh are desired.

The direct mapping of variables may lead to inconsistency between transferred variables and shape functions of the elements. In this case the process of data transfer can be carried out in three steps. In the first step the continuous internal variables are obtained by projecting the Gauss point components to the nodal values. In order to project the values of Gauss points to nodal points, the 3D weighted–SPR method is applied here, as described in previous section. In the second step, the nodal values of internal variables of old mesh are transferred to the nodes of new mesh. For this purpose, we must first determine which element in the old mesh contains the nodal point in the new finite element mesh. The nodal components in the old mesh are then transferred to the nodes of new mesh by applying the old shape functions of old elements and the global coordinates of the new nodes. The components of internal variables at the Gauss points of new mesh are finally obtained by interpolation using the shape functions of elements of the new mesh. These three steps are illustrated schematically in Figure 1. In addition, a transfer operator is employed that transfers the state variables, i.e. displacement field, from the old to a new mesh. This operator includes only the second step of the first operator where the nodal components in the old mesh are transferred to the nodes of new mesh.

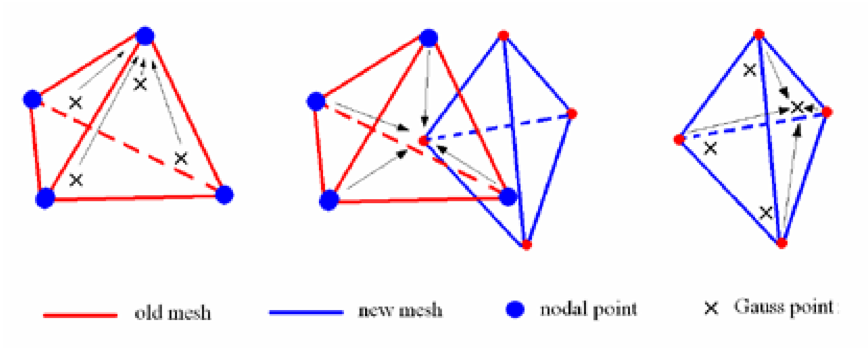

Figure 1: Three-step procedure of the transfer operator

4 NUMERICAL SIMULATION RESULTS

In order to illustrate the accuracy and robustness of the proposed adaptive finite element method in three-dimensional damage mechanics, a classical tensile test of a cylindrical prenotched bar is simulated numerically. The geometry and boundary conditions of the specimen are shown in Figure 2. On the virtue of symmetry, only one-eighth of the problem is modeled. The specimen is subjected to the tensile prescribed displacement at the top edge. The bar is constructed by a low carbon steel in a rolled state with the following material properties; $E = 210$ GPa and $\nu = 0.3$. The strain hardening is considered to be isotropic. The parameters of Lemaitre model for this specimen is taken as $s = 1.0$ and $r = 3.5$ MPa. This specimen was also simulated by de Souza Neto et al. [11] using 2D FE modeling to validate the performance of their constitutive model in damage mechanics. The vertical displacement is applied incrementally in 600 increments of 0.001 mm. The damage evolution is predicted by Lemaitre model until its value reaches to the critical damage value of $D_C = 0.99$.

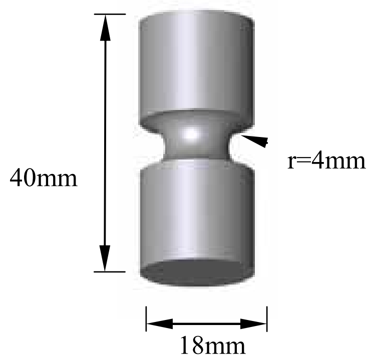

Figure 2: The cylindrical notched specimen; The geometry

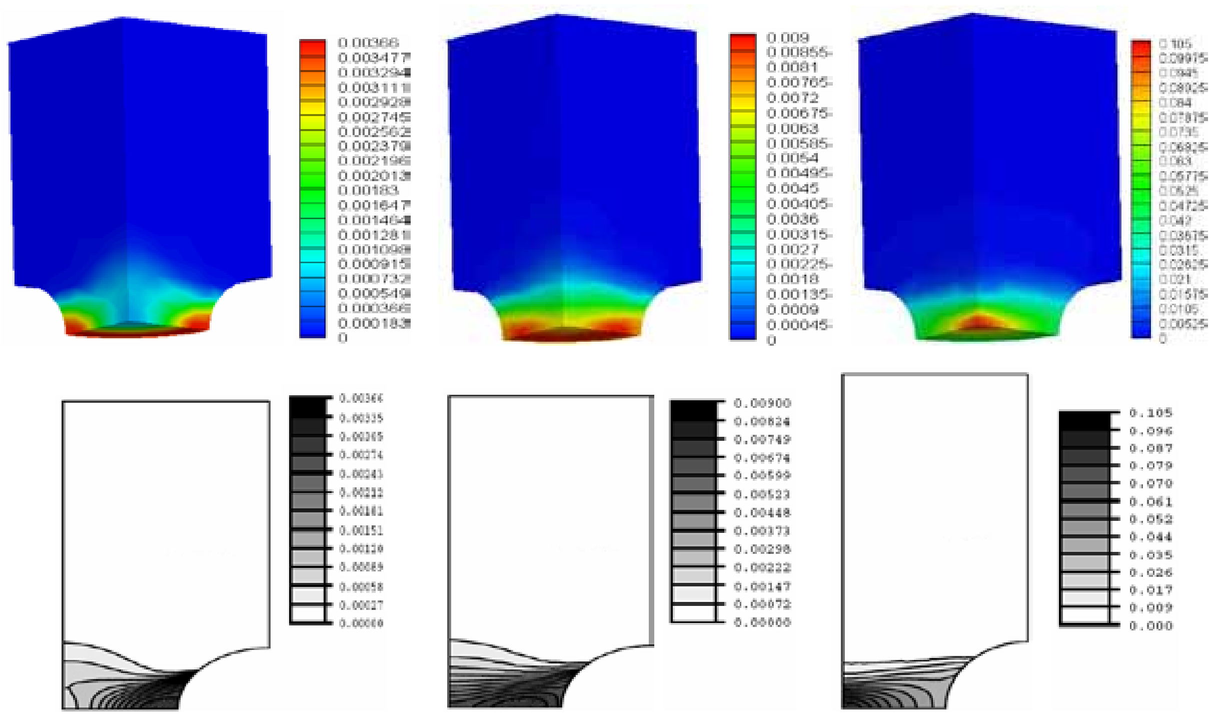

Figure 3: The distribution of damage contours at various load steps; A comparison between the present 3D model and result reported by de Souza Neto et al.[11]; a) $u = 0.051$ mm, b) $u = 0.076$ mm, c) $u = 0.246$ mm

In Figure 3, the distribution of damage contours are shown at three stages and compared wit h those reported by de Souza Neto et al. [11] in two dimensional modeling. It can be seen that the predicted damage contours are in good agreement with those obtained in reference [11]. It is interesting to note that the location of maximum damage is not fixed in the model and moves at different stages of loading. It can be observed that the maximum damage occurs in the outer part of the specimen at the first stages of loading, however – it moves toward the center of the bar by increasing the load. This can be justified by the fact that at early stages of loading the hydrostatic stress is low and the damage evolution is affected by the plastic flow. Thus, the damage grows in outer layers, where the maximum equivalent plastic strain occurs. However, by increasing the load, the hydrostatic stress increases and its effect becomes dominant. Hence, the damage critical point moves toward the center of the bar where the maximum value of hydrostatic stress occurs. In order to control the error of the solution, an adaptive FE mesh refinement is carried out to generate the optimal mesh. The weighted superconvergent patch recovery technique is used with the aim error of 5%. This process is carried out at two steps of 50 and 360, as shown in Figure 4. This figure clearly presents the distribution of elements on the specimen with the growth of damage. In Figure 5, the effect of adaptive strategy can be observed on the estimated error. Obviously, the adaptive mesh refinements result in a reduced estimated error and converge to the prescribed target error.

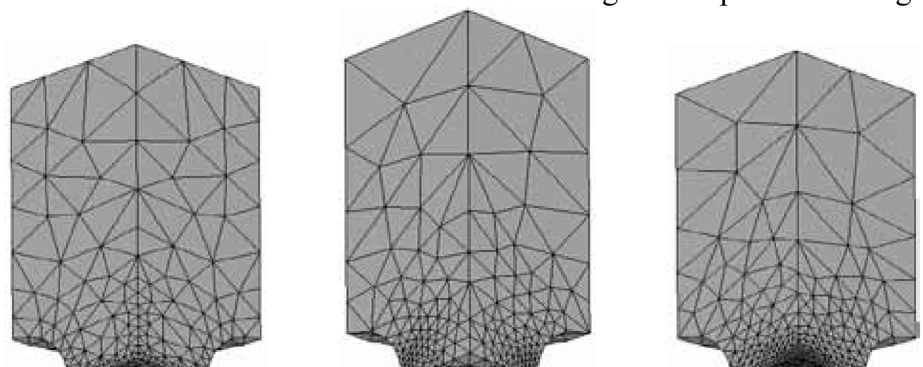

(a) (b) (c)

Figure 4: Adaptive mesh refinement technique for the cylindrical notched specimen; a) Initial FE mesh, b) Adapted mesh at $u = 0.05$ mm , c) Adapted mesh at $u = 0.36$ mm

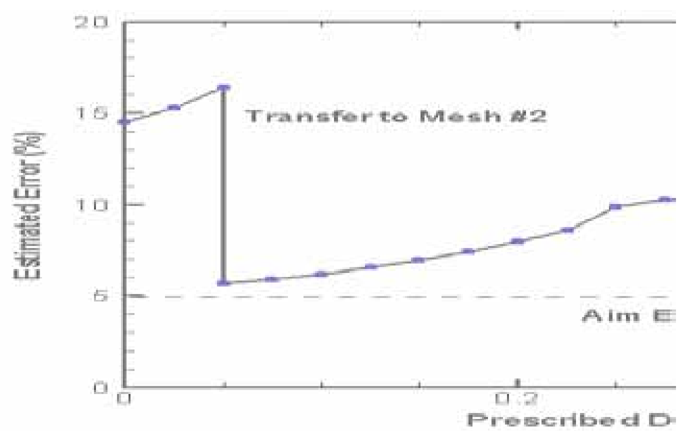

Figure 5: The variation of estimated error with prescribed displacement during adaptive mesh refinement

5 CONCLUSIONS

In the present paper, an adaptive finite element method was presented for the three-dimensional analysis of damage growth and crack initiation. The constitutive modeling was implemented within the framework of continuum damage mechanics. A simplified version of Lemaitre damage model was employed to estimate the damage evolution. The adaptive finite element technique was implemented through the following three stages; an error estimation, adaptive mesh refinement, and data transferring. The error estimation procedure was used based on the Zienkiewicz–Zhu error estimator and a weighted superconvergent patch recovery technique was employed. The accuracy and robustness of proposed computational algorithm in 3D damage mechanics were presented by a numerical example. The results clearly show the ability of the model in capturing the damage growth and crack initiation in complex 3D problem. In a later work, we will show how the proposed technique can be used in a 3D automatic simulation of crack propagation in the fracture of ductile materials.

REFERENCES

[1] Lemaitre, J. A continuous damage mechanics model for ductile fracture, *Journal of Engineering Materials and Technology.* (1985) **107**:83–89.

[2] Kachanov, L.M. Time of the rupture process under creep condition, *Izvestiya Akademii Nauk SSSR*, Otdeleniya Tekhnika Nauk. (1958) **8**:26–31.

[3] Gurson, A.L. Continuum theory of ductile rupture by void nucleation and growth – Part I: Yield criteria and flow rule for porous media, *Journal of Engineering Materials and Technology.* (1977) **99**:2–15.

[4] Lemaitre, J. and Chaboche, J.L. *Mechanics of Solid Materials,* Cambridge University Press, (1990).

[5] Zienkiewicz, O.Z. and Zhu, J.Z. The superconvergent patch recovery and a posteriori error estimates. Part I: The recovery technique, *International Journal for Numerical Methods in Engineering.* (1992) **33**:1331-1364.

[6] Boroomand, B. and Zienkiewicz, O.C. Recovery procedures in error estimation and adaptivity, part II: adaptivity in nonlinear problems of elasto-plasticity behaviour, *Computer Methods in Applied Mechanics and Engineering.* (1999) **176**:127–146.

[7] Khoei, A.R. and Gharehbaghi, S.A. The superconvergence patch recovery and data transfer operators in 3D plasticity problems, *Finite Elements in Analysis and Design.* (2007) **43**: 630–648.

[8] Khoei, A.R., Azadi, H. and Moslemi, H. Modeling of crack propagation via an automatic adaptive mesh refinement based on modified superconvergent patch recovery technique, *Engineering Fracture Mechanics.* (2008) **75**:2921–2945.

[9] Moslemi, H. and Khoei, A.R. 3D adaptive finite element modeling of non-planar curved crack growth using the weighted superconvergent patch recovery method. *Engineering Fracture Mechanics.* (2009) **76**:1703–1728.

[10] Khoei, A.R., Moslemi, H., Majd Ardakany, K., Barani, O.R. and Azadi, H. Modeling of cohesive crack growth using an adaptive mesh refinement via the modified-SPR technique, *International Journal of Fracture.* (2009) **159**:21–41.

[11] de Souza Neto, E.A., Peric and Owen, D.R.J. *Computational Methods for Plasticity: Theory and Applications*, Wiley, UK. (2008).